Journal of Sound and Vibration (1998) **214**(3), 413–430
Article No. sv971512

MODAL ANALYSES AND EXPERIMENTS FOR ENGINE CRANKSHAFTS

Y. KANG, G.-J. SHEEN AND M.-H. TSENG

Department of Mechanical Engineering, Chung Yuan Christian University, Chung Li 32023, *Taiwan, Republic of China*

AND

S.-H. TU AND H.-W. CHIANG

Center for Aviation & Space Technology, Industrial Technology Research Institute, Taiwan, Republic of China

(*Received* 21 *March* 1997, *and in final form* 16 *December* 1997)

This study investigates the coupled modes, including coupled torsional–flexural vibration and coupled longitudinal–flexural vibration, for non-rotating crankshafts which are free–free suspended. The finite element models of those generally used are in two categories: beam elements and solid elements. By using these two models the natural frequencies and mode shapes of two crankshafts are determined by the finite element method (FEM) and compared with experimental data from modal testing. The accuracy and validity of the analytical approaches are verified. The results show that the solid element is more appropriate than the beam element in the modal analysis of crankshafts.

1. INTRODUCTION

Presently, the rotor–bearing systems utilized for modelling rotating machinery and their mounting structures, for example, electric motors, turbomachinery, transmission shafts, propellers, etc., are commonly analyzed by the finite element method. Computations of natural frequencies, mode shapes, critical speeds, steady state responses, and transient responses play important roles in the design, identification, diagnosis, and control of rotor–bearing systems. Thus, an accurate prediction for the dynamic characteristics of a rotor–bearing system using FEM is essential for modern equipment.

The finite element procedures developed for rotor–bearing systems are directed toward generalizing and improving the shaft model proposed by Ruhl and Booker [1]. Nelson and McVaugh [2], Zorzi and Nelson [3] utilized finite beam element models to formulate the dynamic equation for a linear rotor system and determine the stability and steady state responses. The beam formulations based primarily on Timoshenko's assumptions have been given by Thomas *et al*. [4]. Özgüven and Özkan [5] and Nelson [6] further developed the finite element model by including the effects of rotary inertia, gyroscopic moments, shear deformation, and internal damping. Tapered beam elements have been developed by Rouch and Kao [7] and Greenhill *et al*. [8] to model a linearly varying diameter along the beam length. Stability and steady state responses of asymmetric rotors with a flexible shaft have been studied by Genta [9]. The effects of both deviatoric inertia and stiffness due to an asymmetric shaft and disk have been studied by the finite element method in research by Kang *et al*. [10].

0022–460X/98/280413 + 18 $30.00/0

Moreover, many mechanical systems such as turbine blades, aircraft propellers, robot arms and engine crankshafts, which are perpendicular to a rotating axis, can be modelled by a radial rotating beam element. Nagaraj and Shanthakumar [11] used the Galerkin method, together with an eighth-order polynomial, for solving a problem concerning a rotating beam without a hub. Putter and Manor [12] presented a six-degree-of-freedom element for a rotating radial cantilever beam to allow inclusion of a shroud mass. Hoa [13] presented a finite element formulation for a uniform rotating beam with a tip mass. Khulief and Yi [14] developed a finite element formulation representing the vibrational response of a uniform rotating beam with a tip mass during flapping and lead–lag motion. Their formulation accounts for the centrifugal force field and centripetal acceleration effects. Yokoyama [15] developed a finite element procedure for determining the free vibration characteristics of rotating uniform Timoshenko beams. The effects of hub radius, setting angle, shear deformation, and rotary inertia on the natural frequencies of the

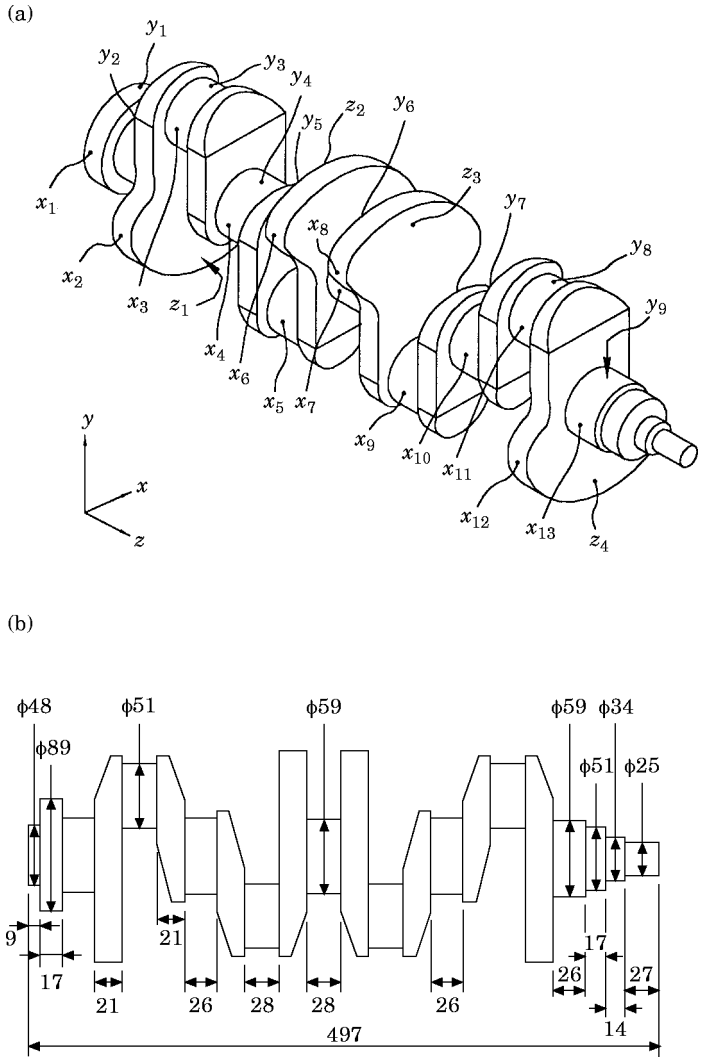

Figure 1. Crankshaft of an in-line four-cylinder engine; (a) spatial view and arrangement of measurement points and excitation points, ◀—— excitation point; ●——, measurement point; (b) dimension details (in mm).

rotation beams have been examined. Magari *et al*. [16] developed a rotating blade finite element with coupled bending and torsion. Khulief [17] derived explicit expressions for the finite element mass and stiffness matrices using a consistent mass formulation for the vibration of a rotating tapered beam. Bazoune and Khulief [18] developed a finite element for vibration analysis of rotating tapered Timoshenko beams.

Bagci and Rajavenkateswaran [19] utilized a spatial finite line element method in an analysis of rotors, including crankshafts. Smaili and Khetawat [20] proposed a spatial four-node beam element based on Timoshenko's theory for the modelling of crankshafts.

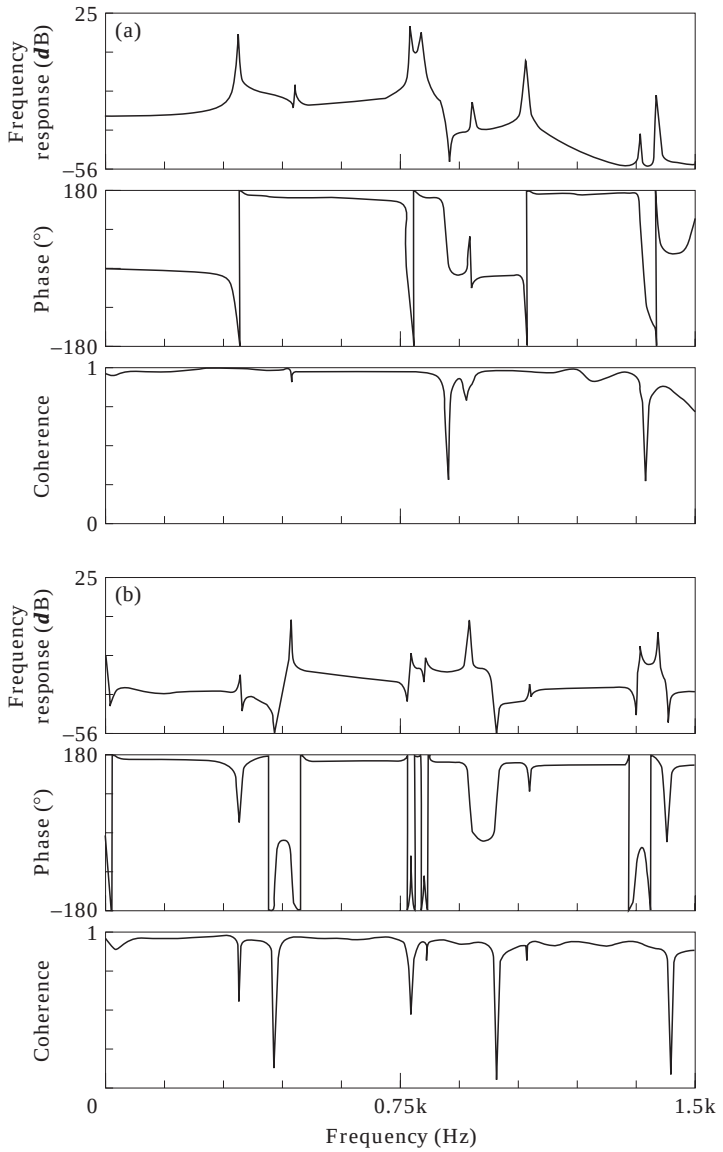

Figure 2. Examples of modal testing for a four-cylinder crankshaft (a) excitation at point z_1 in the z- direction, and measurement at point y_9; (b) excitation at point y_9 in the y-direction, and measurement at point x_{11}.

Geradin and Kill [21] derived a three-dimensional finite element for modelling flexible rotors, because it produces good estimation in stepped and tapered shaft analyses. Stephenson *et al*. [22] showed an excellent agreement between the measured frequencies and the frequencies calculated by using an axisymmetric solid finite element model. Stephenson and Rouch [23] presented axisymmetric solid finite elements with matrix reduction in modelling a rotating shaft.

The complex spatial nature of engine crankshafts makes the solid element approach an attractive one for determining their coupled flexural, torsional, and longitudinal vibration modes. This study models practical crankshafts by using both a tetrahedron element and a beam element and compares the analytical results with data from modal testing. For comparing the analytical results with experimental data, two crankshafts from a four-cylinder in-line engine and a six-cylinder V-shaped engine are used. The comparison shows that the eigensolutions for crankshafts with a beam element model are not favorably compatible with the modal testing results. Not only are some important modes lost in the analytical results, but also the corresponding frequencies are quite different from the modal testing ones. Although the time consumption is vast for modelling and computation, the results obtained from solid element models perform favorably in being consistent with the experimental data.

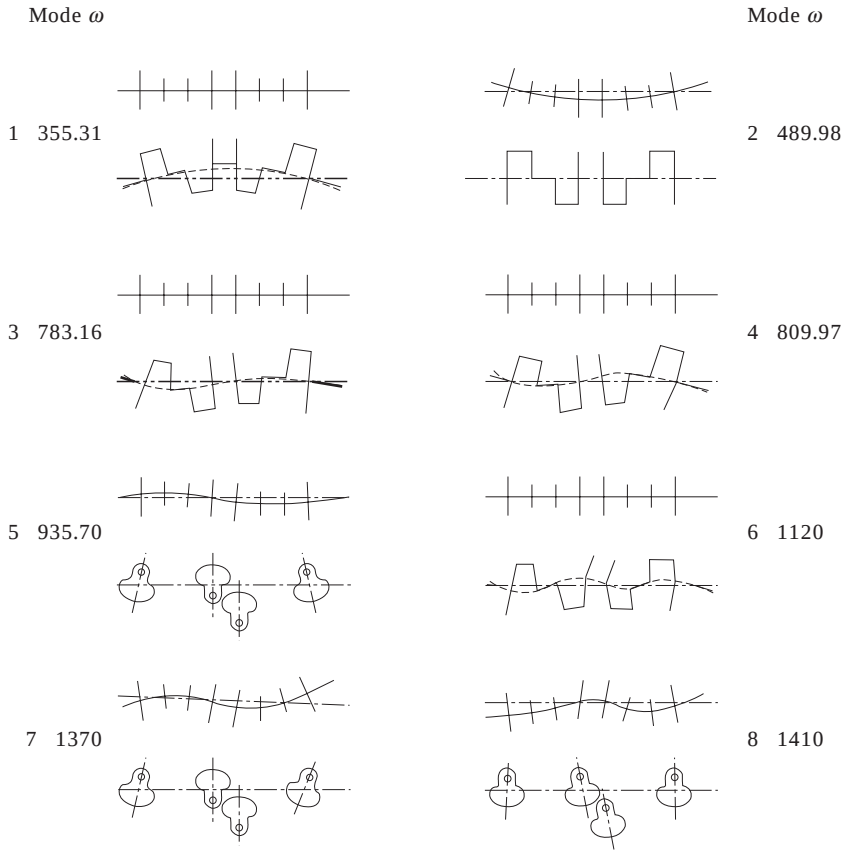

Figure 3. Natural frequencies and mode shapes for the crankshaft of a four-cylinder engine shown in Figure 1.

2. MODAL TESTING

A crankshaft of a four-cylinder in-line engine is utilized for testing, as shown in Figure 1, in which the exciting points and measuring points are indicated by the symbols ▼ and ●, respectively. The crankshaft is suspended with rubber bands to simulate free–free boundary conditions for modal testing. Exciting the crankshaft with an impactor or hammer at all impact points and measuring the responses of all measuring points, one obtains the transfer function of the crankshaft by means of the FFT analyzer (HP3566A).

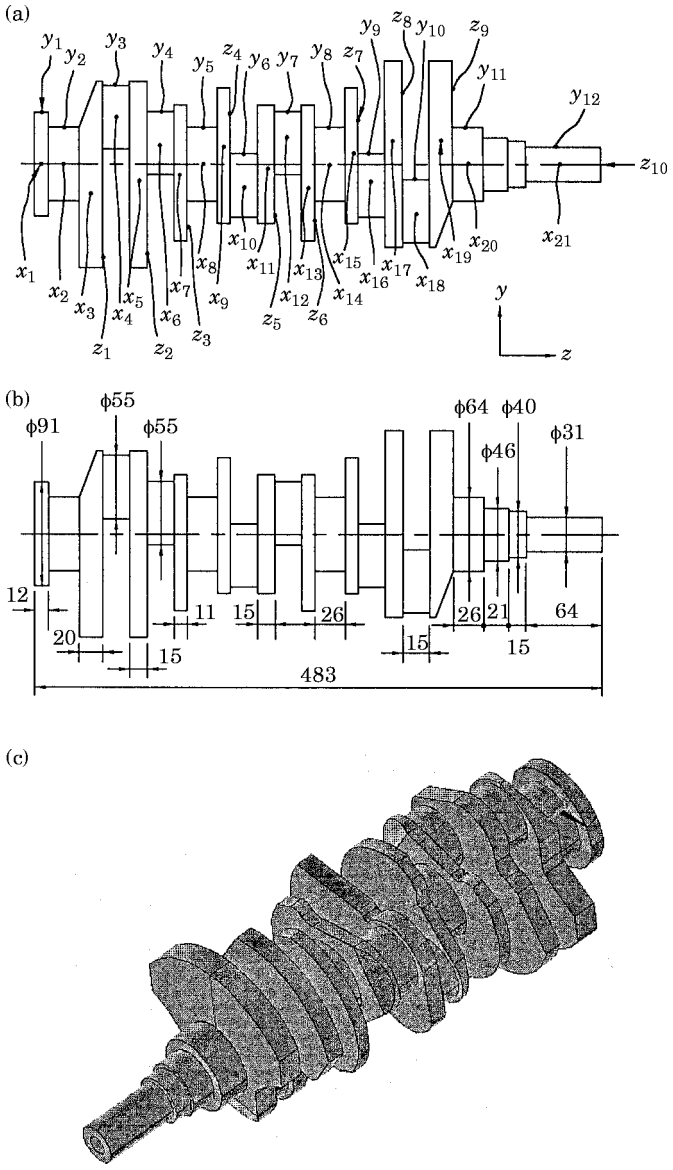

Figure 4. Spatial view and dimension details of a V6-cylinder crankshaft; (a) arrangement of measurement and excitation points; (b) dimension details (mm); (c) spatial view.

Two spectra of frequency responses from this crankshaft are shown in Figures 2(a) and 2(b).

From the spectra, the natural frequencies of the first eight modes, which occur at 355·31 Hz, 489·98 Hz, 783·16 Hz, 809·97 Hz, 935·70 Hz, 1120·0 Hz, 1370·0 Hz, and 1410·0 Hz and correspond to each of the peaks shown in Figures 2(a) and 2(b) can be observed. By using analyses from the SIMO technique, one obtains more shapes of the crankshaft, shown in Figure 3. Actually, the vibrations of each of the modes in x, y, z, θ_x, θ_y, θ_z are all coupled with longitudinal, torsional, and flexural vibrations. Each mode can be categorized into its prevailing vibrations as: first and second modes caused by flexural vibration in two principal axes; third, fourth and sixth modes caused by coupled

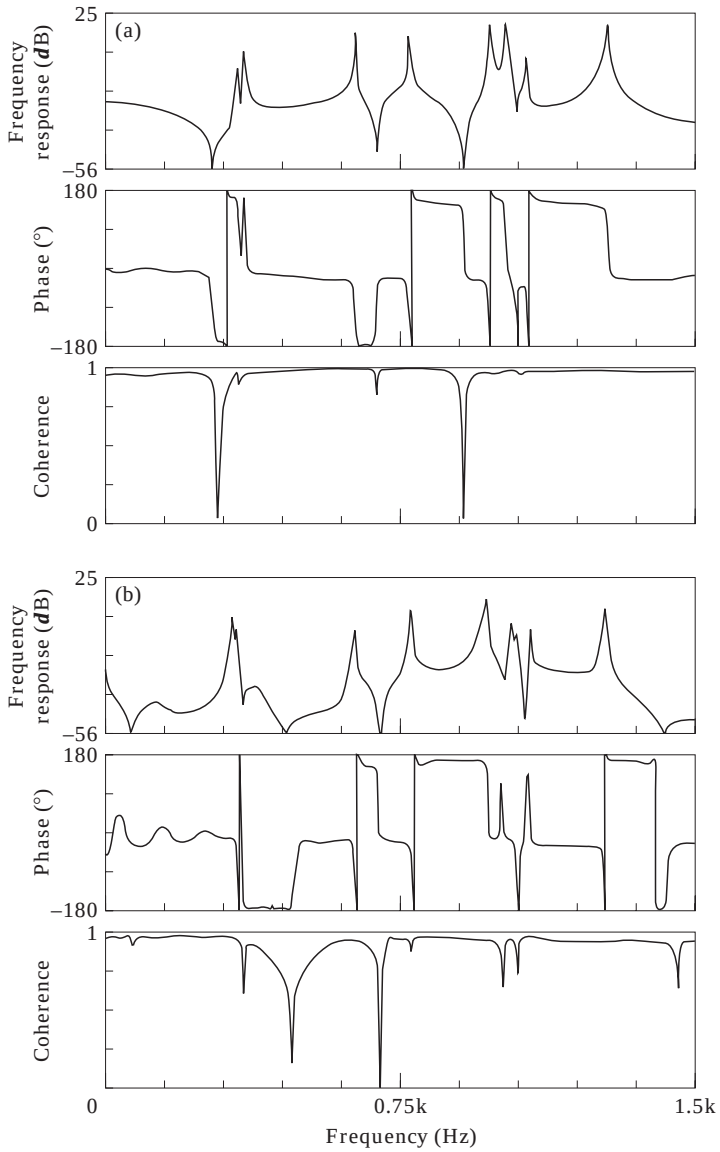

Figure 5. Examples of modal testing for a six-cylinder crankshaft (a) excitation at point z_7 in the z direction, and measurement at point y_1; (b) excitation at point x_{19} in the x direction, and measurement at point y_1.

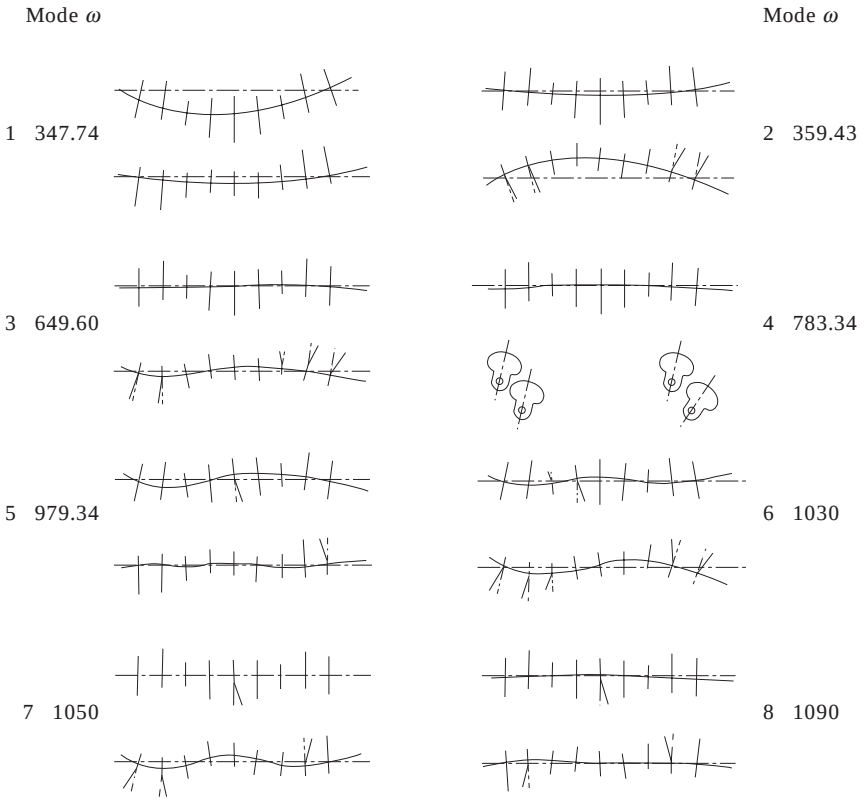

Figure 6. Natural frequencies and mode shapes for the crankshaft of a V6 engine in Figure 4.

longitudinal–flexural vibration; fifth, seventh and eight modes caused by coupled torsional and flexural vibrations. In each mode the longitudinal vibrations are the displacements of cranks and counterbalances (in the axial direction z); the flexural vibrations are the lateral displacements (in directions x or y) or the angular displacements (in directions θ_y or θ_x) of the connecting pins and journals; the torsional vibrations are the angular displacements of connecting pins (in the rotating axis θ_z).

Another crankshaft from a six-cylinder V-shaped engine, shown in Figure 4, is tested for further verification, in which the exciting points and measuring points are indicated by the symbols ▼ and ● respectively. With the same instruments and process, one obtains

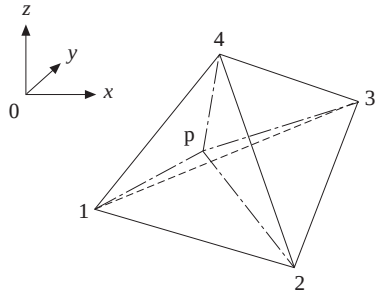

Figure 7. Volume co-ordinates for a tetrahedron. v_1, P234; v_2, P341; v_3, P412; v_4, P123.

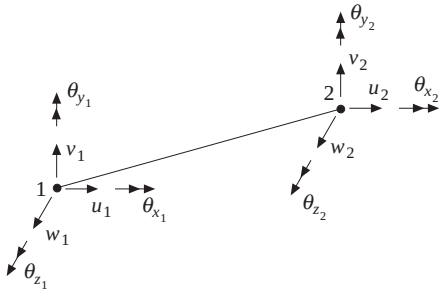

Figure 8. 2-node 3D space beam element.

the transfer function. Figures 5(a) and 5(b) show the two frequency responses from the same measuring point with excitation at two different typical points. From these figures, one obtains the natural frequencies of the first eight modes, which are 347·74 Hz, 359·43 Hz, 649·60 Hz, 783·34 Hz, 979·34 Hz, 1030·0 Hz, 1050·0 Hz, and 1090·0 Hz, individually. By using the data from the FFT analyzer, the mode shapes of this crankshaft are obtained and shown in Figure 6.

3. COMPUTATIONAL MODAL ANALYSES

The crankshafts are modelled with two approaches involving the solid elements and the beam elements, respectively, but the internal damping is disregarded.The degrees of

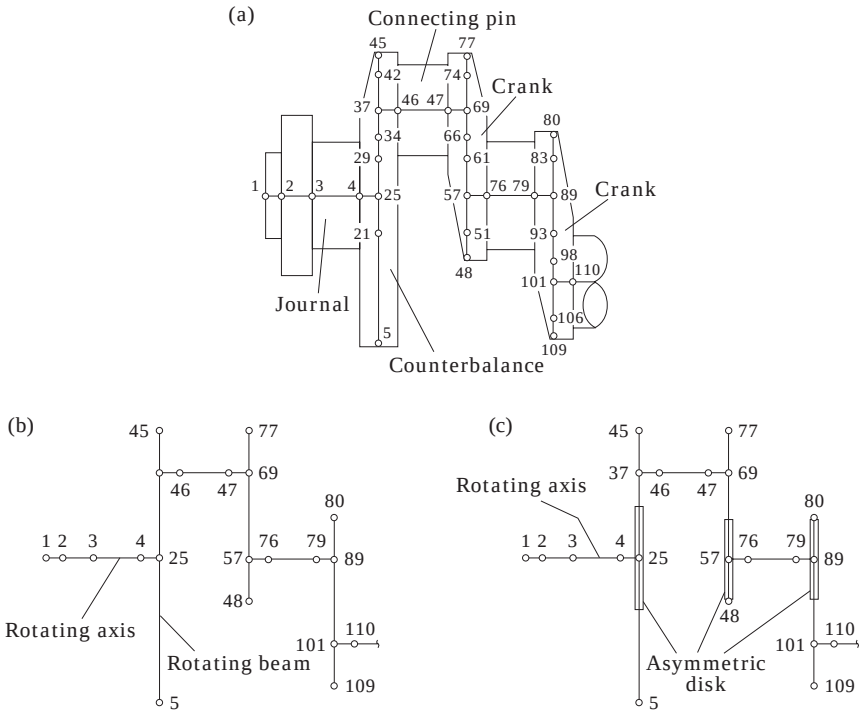

Figure 9. Modelling of a four-cylinder crankshaft by beam elements (a) typical part (b) basic model (c) modified model.

TABLE 1

Comparisons of natural frequencies obtained by using stiff beam modelling for the four-cylinder crankshaft (Hz)

Mode Order	Modal Testing	Model 1	Error (%)	Model 2	Error (%)	Model 3	Error (%)
1	355·31	201·98	43·15	201·26	43·36	362·70	2·08
2	489·98	496·15	1·26	903·03	84·30	955·26	94·96
3	783·16	449·05	42·67	500·57	36·08	838·93	7·12
4	809·97	–	–	–	–	–	–
5	935·70	990·27	5·83	1259·6	34·62	2387·5	155·16
6	1120	654·37	41·57	1001·4	10·59	1257·8	12·30
7	1370	1385·8	1·15	2026·9	47·95	2870·2	109·50
8	1410	2116·3	50·09	2241·2	58·95	4628·6	228·27

freedom (DOF) of a tetrahedral element provided by the ANSYS library [24], as shown in Figure 7, are defined by

$$\{\mathbf{q}^e\} = [u_1, v_1, w_1, \ldots, u_4, v_4, w_4]^T$$

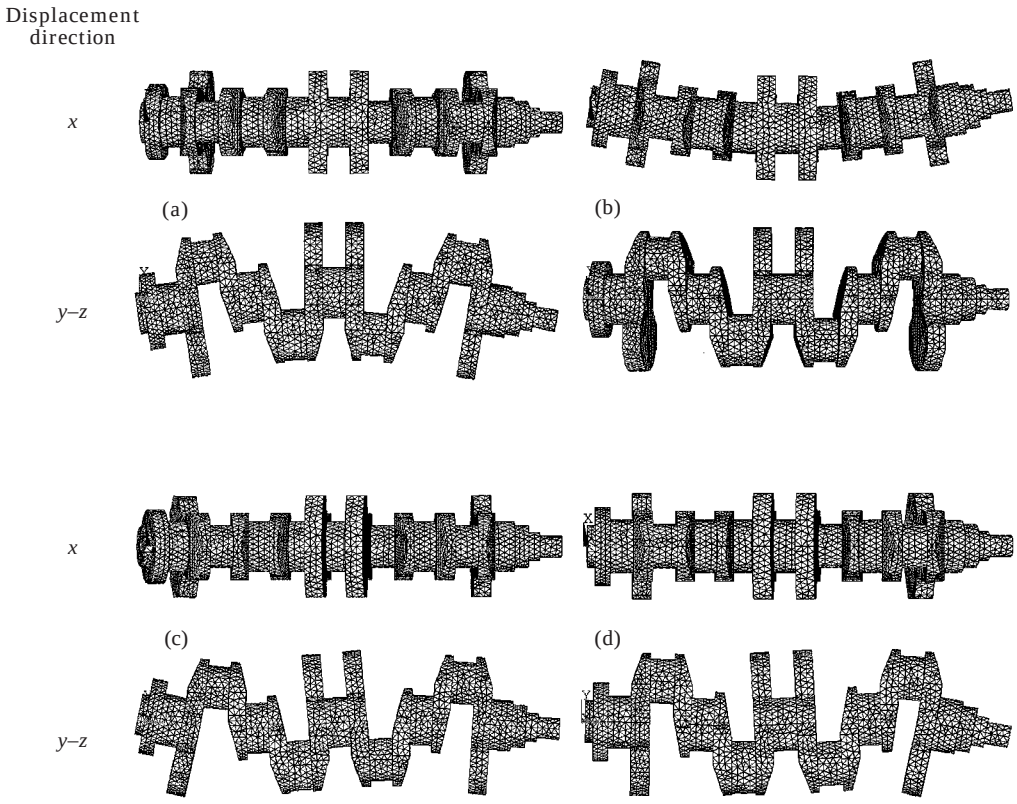

Fig. 10(a–d)—*Caption on p*. 422

where u_i, v_i and w_i are node displacements in the Cartesian co-ordinates of the fixed reference frame. For a beam element also provided by the ANSYS library, as shown in Figure 8, the DOF are defined by

$$\{\mathbf{q}^e\} = [u_1, v_1, w_1, \theta_{x1}, \theta_{y1}, \theta_{z1}, u_2, v_2, w_2, \theta_{x2}, \theta_{y2}, \theta_{z2}]^T$$

The motion equations of a free–free suspended crankshaft modelled by both of the two previous elements in a fixed reference frame have a similar form as:

$$[\mathbf{M}]\{\ddot{\mathbf{q}}\} + [\mathbf{K}]\{\mathbf{q}\} = \{\mathbf{0}\}$$

where [**M**] and [**K**] are constant matrices and $\{\mathbf{q}\}$ represents the DOF in the global system. ANSYS offers six methods for mode extraction: subspace method, block Lanczos method, reduced method, power dynamics method, unsymmetric method, damped method. The first three methods are applicable to this study and described briefly in the following:

The generalized Jacobi iteration algorithm is used by the subspace method. This method is typically used in cases where high accuracy is required because is uses the full [**M**] and [**K**] matrices. However, the subspace method is slower than the reduced method.

The Lanczos recursion performed with a block of vectors is used by the block Lanczos method. It is powerful when searching for eigenfrequencies.

The householder-bisection-inverse iteration is used by the reduced method to calculate the eigenvalues and eigenvectors. It is relatively fast because it works with a small subset

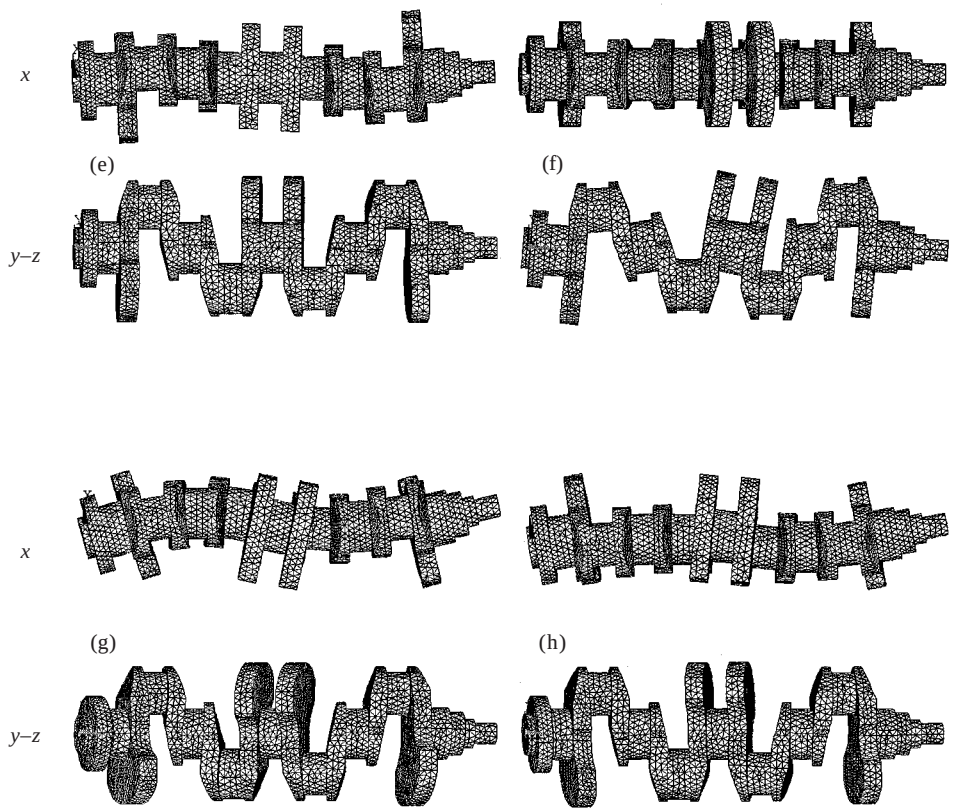

Fig. 10(e–h)

Figure 10. Mode shapes of a four-cylinder crankshaft (analysis by using a solid model). Mode shapes: (a) mode 1; (b) mode 2; (c) mode 3; (d) mode 4; (e) mode 5; (f) mode 6; (g) mode 7; (h) mode 8.

TABLE 2

Comparisons of natural frequencies obtained by using solid element modelling for the four-cylinder crankshaft (Hz)

	Subspace method		Block Lanczos method		Reduced method (MDOF = 100)	
Mode Order	Natural frequency	Error (%)	Natural frequency	Error (%)	Natural frequency	Error (%)
1	354·43	0·26	354·43	0·26	354·77	0·20
2	486·11	0·79	486·11	0·79	487·26	0·48
3	738·49	5·70	738·49	5·70	741·95	5·42
4	786·22	2·88	786·22	2·88	790·91	2·15
5	875·81	6·40	875·81	6·40	880·48	5·91
6	1062·1	3·76	1062·1	3·76	1073·6	3·94
7	1294·8	5·49	1294·8	5·49	1309·9	4·28
8	1334·0	5·39	1334·0	5·39	1352·1	3·92

of degrees of freedom called master degrees of freedom (MDOF). Using MDOF leads to an exact [**K**] matrix but an approximate [**M**] matrix. The accuracy of the results, therefore, depends on how well [**M**] is approximated, which in turn depends on the number and location of MDOF. In the ANSYS package, it permits the user to select the MDOF, or the program to select them automatically, or any combination of these two options. If the structure has an irregular mass distribution, the automatically selected MDOF may be concentrated totally in the high mass regions, in which case the manual selection of some MDOF should be used. As the structure of crankshafts, the MDOF can be selected totally by the ANSYS program itself with good predictions in result. Empirically, the number of the MDOF should usually be at least equal to twice the number of modes of interest to achieve a better approximate [**M**] matrix and avoid error predictions in higher modes.

3.1. CASE STUDY FOR A FOUR-CYLINDER CRANKSHAFT

The available literature on numerical analysis of crankshafts is mainly concerned with modelling by beam elements. The advantages of modellng by beam elements include

TABLE 3

Comparisons of natural frequencies obtained by using different number of master DOF (MDOF) in reduced method (Hz)

Mode Order	MDOF 14	Error (%)	MDOF 30	Error (%)	MDOF 100	Error (%)	MDOF 200	Error (%)
1	360·15	1·36	356·42	0·31	354·77	0·20	354·65	0·19
2	526·79	7·51	502·10	2·47	487·26	0·48	486·86	0·64
3	831·88	6·22	753·92	3·73	741·95	5·42	739·78	5·54
4	1066·6	31·68	808·56	0·17	790·91	2·15	789·13	2·57
5	1103·9	17·98	920·02	1·68	880·48	5·91	878·11	6·15
6	1881·0	67·95	1113·9	0·54	1073·6	3·94	1068·2	4·63
7	2943·2	114·8	1443·3	5·35	1309·9	4·28	1303·7	4·84
8	3643·7	158·4	1601·0	13·55	1352·1	3·92	1343·8	4·70
Computer time (min)	210		218		243		494	

greater ease in preprocessing, faster computation, and less computer memory. In this case, the cranks and counterbalances are modelled by radial rotating beams; the journals are modelled by spinning beams; the connecting pins are modelled by whirling beams. ANSYS provides a taper beam element, Beam44, for the analysis of the aforementioned three types of beams.

To simulate a practical crankshaft, three models are proposed for crankshaft modelling: (1) the basic model: all segments of the crankshaft are considered as spatial beams and the nodes of the beams are along the geometrical centers of the segments, as ilustrated in Figure 9(a); and this model is simplified into a basic finite element model, shown in Figure 9(b); (2) the first modified model: the stiffness of the cranks and the counterbalances is considered as beam stiffness, while the inertia thereof is considered as asymmetric plates of zero thickness, shown in Figure 9(c); the entities of the inertia matrix of an asymmetric plate are presented in the report by Kang *et al*. [10]; (3) the second modified model: by using stiffening beams to care for the "cross sections remain plane" condition of the junctions of journals and connecting pins or the junctions of counterbalances and cranks (Beams from Node 21 toward Node 29 or beams from Node 34 toward Node 42 in Figure 9(a), for example). According to the theory proposed by Rao [25], the stiffness of the beam elements which are close to the junctions of the cranks or counterbalances is strengthened, as the elements of nodes 4–25, 37–46, 47–69, 57–78, 79–89 shown in Figures 9(a)–9(c).

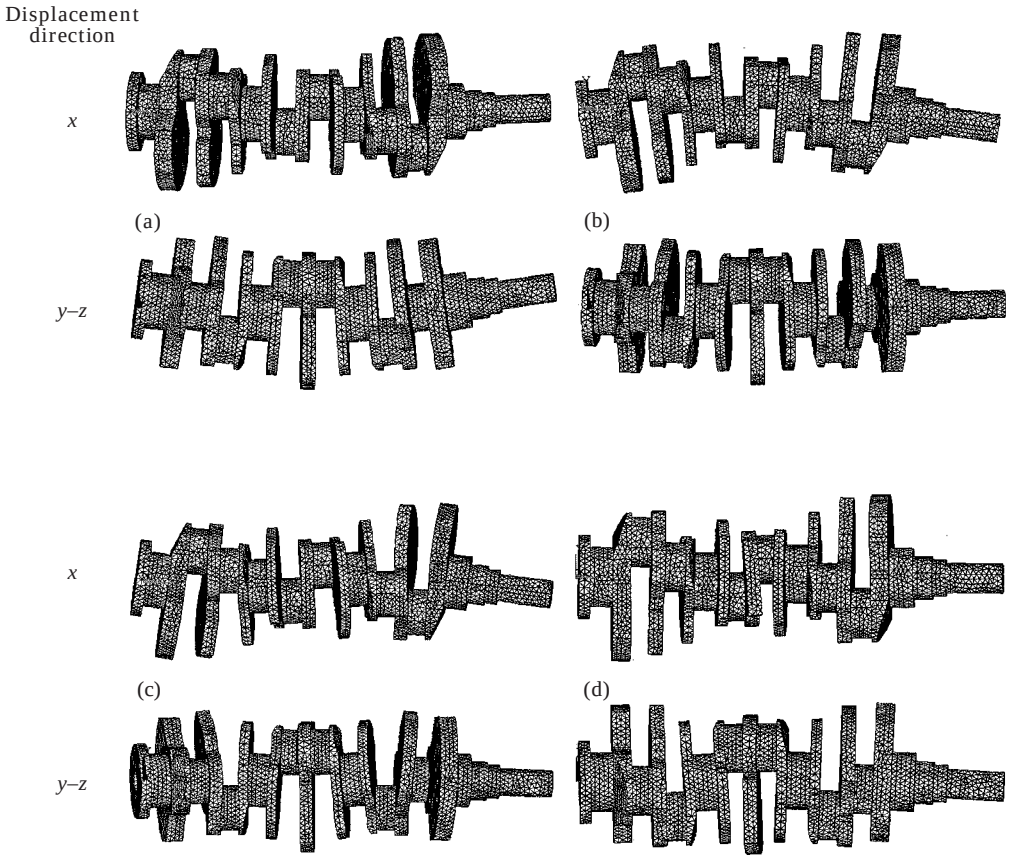

Fig. 11(a–d)—*Caption on p*. 425.

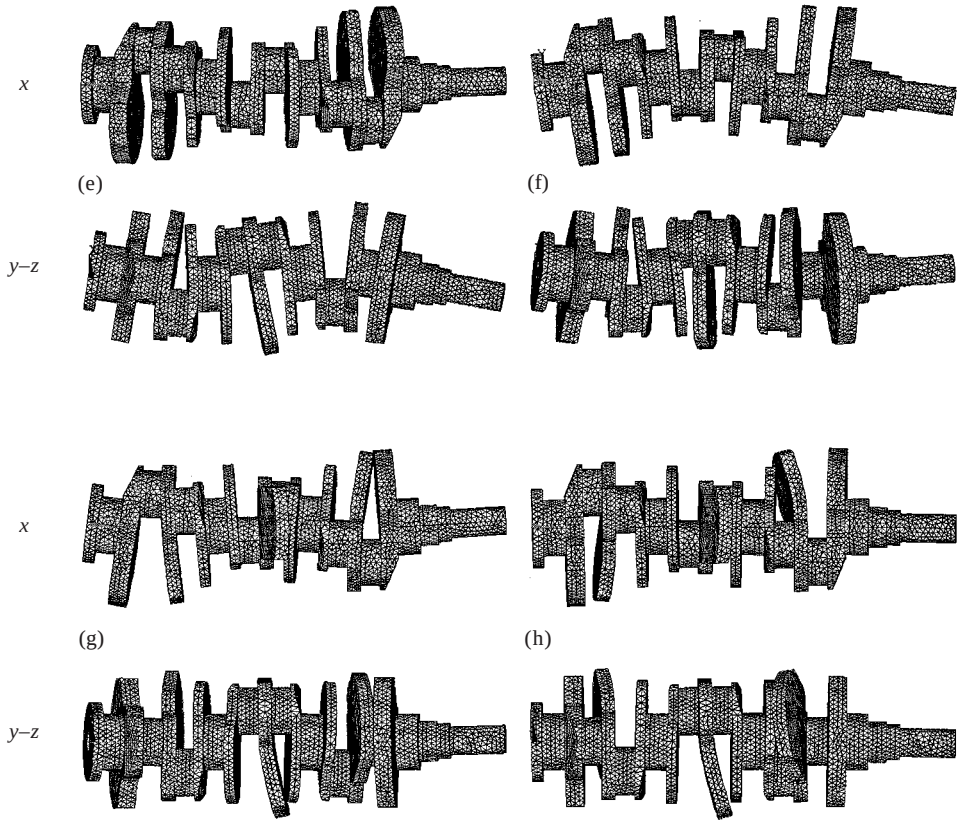

Fig. 11(e–h).

Figure 11. Mode shapes of a six-cylinder crankshaft (analysis by using a solid model). Mode shapes: (a) mode 1; (b) mode 2; (c) mode 3; (d) mode 4; (e) mode 5; (f) mode 6; (g) mode 7; (h) mode 8.

A four-cylinder crankshaft shown in Figure 1 is modelled by the proposed three models and analyzed by using the ANSYS package, in which a counterbalance is meshed into 40 rotating beams and a crank is meshed into 29 rotating beams along the geometrical center thereof; the journals and the connecting pins are modelled as spinning beams and whirling beams respectively, according to the illustration of Figure 9(a). These models are analyzed by using the subspace method in ANSYS package. The natural frequencies and mode

TABLE 4

Comparisons of natural frequencies obtained from modal testing and ANSYS analysis for the six-cylinder crankshaft (Hz)

Mode order	Modal testing	Subspace method	Error (%)
1	347·74	357·94	2·93
2	359·43	366·41	1·94
3	649·60	657·46	1·21
4	783·34	766·78	2·11
5	979·34	904·50	7·64
6	1030	1035·4	0·52
7	1050	1077·9	2·66
8	1090	1167·1	7·07

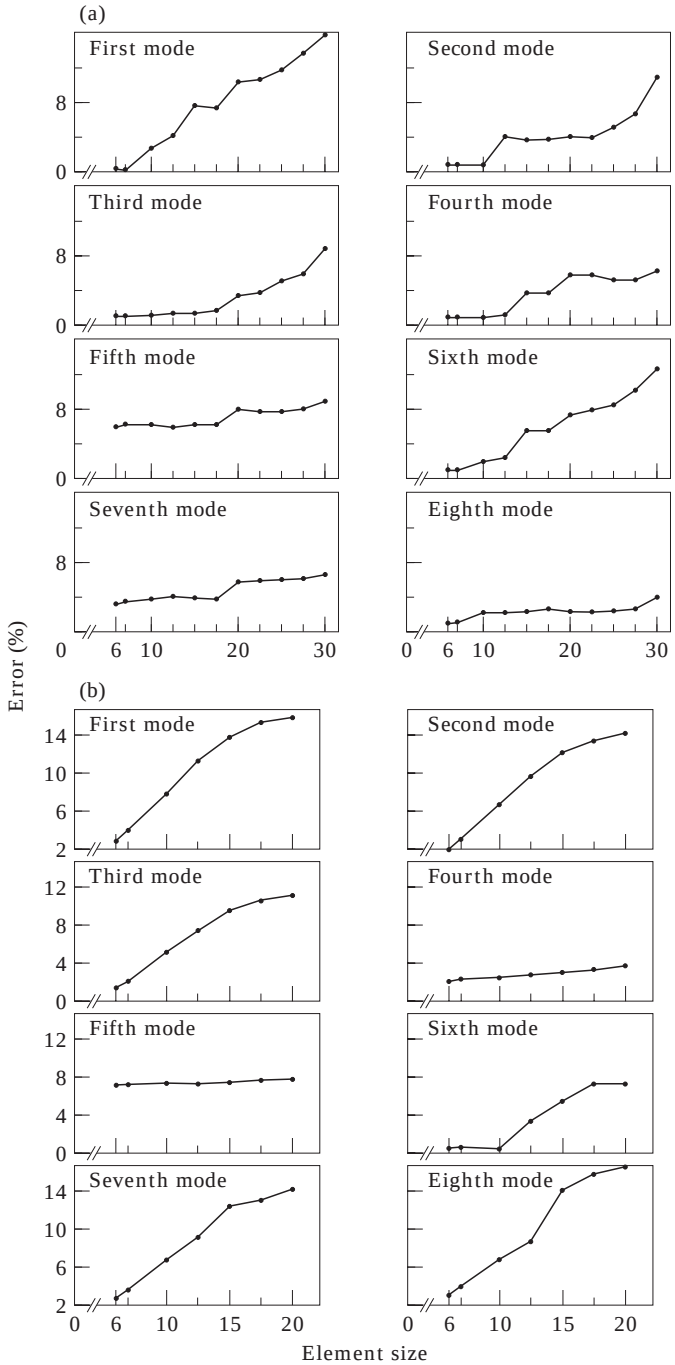

Figure 12. Error percentages of natural frequencies of numerical results: (a) four-cylinder crankshaft; (b) six-cylinder crankshaft.

shapes of the first twenty modes are obtained and each mode shape has been checked carefully with the mode shapes from the modal testing, shown in Table 1. The Table indicates that the natural frequencies of the analytical results are very different from the tested results. Also, the mode orders from analytical results are different from those

of the tested results. Meanwhile, the fourth mode of the modal testing is not present in all three analyses.

The same four-cylinder crankshaft is also analyzed by the ANSYS solid element, Solid72, using the subspace, the block Lanczos and the reduced methods to extract the first eight modes. The crankshaft is meshed automatically by the ANSYS package with the element size from 0·02–0·005 m. In the reduced method, the number of master DOF is set to 100 and the DOF are selected by the program itself. The mode shapes and mode orders obtained from the three methods are very similar. Thus, mode shapes obtained from the subspace method have been show in Figures 10(a)–10(h). Each illustration has the top view and the front view to indicate the vibration displacements and the patterns of mode shapes. These illustrations show a good correlation with the tested results. The differences in the natural frequencies between experimental and analysis results are shown in Table 2. Although the reduced method seems to have the best prediction, from this table, all the three methods are very close in results. One does not conclude that the reduced method has the most precise estimation, because some dimension details (such as forged segments and lubrication vents) are neglected in the present modeling.

From the comparisons of Table 1 and Table 2, one may state that the beam theory is probably not appropriate for crankshafts and the solid analyses have better predictions than the beam analyses do.

Table 3 shows the mode frequency and computer times of different number of master DOF in the reduced method, which indicates that the greater the number of master DOF set, the more accurate the mode frequency obtained and more computer time required. The number of master DOF (100) is a favorable selection in this case study, for the results converge well and the computation time not much greater than that with a smaller number of master DOF.

3.2. CASE STUDY OF A SIX-CYLINDER CRANKSHAFT

Another case of a six-cylinder crankshaft in a V-shaped engine, shown in Figure 4, is analyzed by using the Solid72 model with the subspace method. The natural frequencies and mode shapes of the first eight modes are shown in Figure 11. The shapes show that the first mode is due to pure bending vibration, the fourth mode is due to coupled torsional-lateral vibration, and the other six modes are due to coupled longitudinal–lateral vibration. These analytical results are compatible with the mode shapes which were determined by modal testing.

TABLE 5

Computer times for the four-cylinder crankshaft

Element size (m)	Node no.	Element number	Computer time (min.) Subspace method	Block Lanczos method	Reduced method (MDOF = 100)
0·005	26851	119940	full disk	697	full disk
0·006	16876	72113	921	270	631
0·007	11285	46254	468	139	243
0·01	4998	18714	103	44	62
0·0125	3430	12220	51	27	31
0·015	2334	7942	31	24	24
0·0175	1913	6205	23	17	20
0·02	1501	4629	21	15	18

TABLE 6

Computer times for the six-cylinder crankshaft by using subspace method

Element size (m)	Node no.	Element no.	Computer time (min)
0·006	18675	74935	1232
0·007	13520	53038	623
0·01	5718	19644	119
0·0125	4095	13631	76
0·015	2290	6797	28
0·0175	1979	5682	23
0·02	1604	4550	18

Comparing the natural frequencies of the numerical results with the experimental data, shown in Table 4, a good correlation can be obtained, except for the fifth and eighth modes, which have an error of about 7%.

4. COMPUTER TIME AND CONVERGENCE

A crankshaft analyzed by solid element models essentially involves the choice of element size. If the element size is too large, it leads to a large error in the result. Contrarily, if the element size is too small, it gives a very precise result but demands more computer time and memory and may also cause a truncation error. By using the subspace method, the influences of element size on the error percentage of the natural frequencies are compared and shown in Figures 12(a) and 12(b) for the four-cylinder and six-cylinder crankshafts respectively. From both figures, one observes that if the element size is reduced to approximately 6 mm, the analytical results converge to the experimental results. Tables 5 and 6 show the computation time for extracting the first twenty modes of the two crankshafts in different element sizes using a Pentium586-166 personal computer with 96MB RAM and a 4GB HD. Table 5 indicates that the block Lanczos method is the most efficient when mode extracting and the reduced method always takes less computer time than the subspace method. Furthermore, the subspace method requires more disk space and the reduced method is used to find only a few modes of larger models. However, the accuracy of its frequencies depends on the master DOF selected.

5. CONCLUSIONS

The free vibration of a crankshaft is in a sophisticated form which includes longitudinal–flexural vibrations, torsional–flexural vibrations, or vibrations coupled with three of longitudinal, flexural and torsional together. It is difficult to simulate such vibration characteristics using a beam element; however, the use of solid element modelling in crankshaft analysis produces much better estimation results.

In this study two practical crankshafts, one a four-cylinder in-line and the other a six-cylinder V-shaped, have been utilized for numerical analysis and modal testing; and the results of the three modelling methods have been compared with the modal testing results. When the crankshafts are modelled by beam elements, no agreement in natural frequency estimations can be obtained. When the crankshafts are modelled by solid elements, the first eight modes obtained have errors in natural frequencies within 3%, except for a few which have about 5%.

In summary, the beam elements model is usable in analyses of most rotor–bearing systems and radial rotating configurations, but it is not practical for a complex

configuration of an engine crankshaft. Comparatively, the solid element model correlates with the results of modal testing.

ACKNOWLEDGMENTS

This study was supported by the National Science Council of the Republic of China under grant number NSC 86-2612-E033-001.

REFERENCES

1. R. Ruhl and J. F. Booker 1972 *ASME Journal of Engineering for Industry* **94**, 128–132. A finite element model for distributed parameter turbo–rotor systems.
2. H. D. Nelson and J. M. McVaugh 1976 *ASME Journal of Engineering for Industry* **98**, 593–600. The dynamics of rotor–bearing systems using finite elements.
3. E. S. Zorzi and H. D. Nelson 1977 *ASME Journal of Engineering for Power* **99**, 71–76. Finite element simulation of rotor–bearing systems with internal damping.
4. D. L. Thomas, J. M. Wilson and R. R. Wilson 1973 *Journal of Sound and Vibration* **31**, 315–330. Timoshenko beam finite elements.
5. N. H. Özgüven and L. Z. Özkan 1984 *ASME Journal of Vibration*, *Acoustics*, *Stress*, *and Reliability in Design* **106**, 72–79. Whirl speeds and unbalance response of multi-bearing rotors using finite elements.
6. H. D. Nelson 1980 *ASME Journal of Mechanical Design* **102**, 793–803. A finite rotating shaft element using Timoshenko beam theory.
7. K. E. Rouch and J. S. Kao 1979 *Journal of Sound and Vibration* **66**, 119–140. A tapered beam finite element for rotor dynamics analysis.
8. L. M. Greenhill, W. B. Bickford and H. D. Nelson 1985 *ASME Journal of Vibration*, *Acoustics*, *Stress*, *and Reliability in Design* **107**, 421–427. A conical beam finite element for rotor dynamics analysis.
9. G. Genta 1988 *Journal of Sound and Vibration* **124**, 27–53. Whirling of unsymmetrical rotors: a finite element approach based on complex co-ordinates.
10. Y. Kang, Y. P. Shih and A. C. Lee 1992 *ASME Journal of Vibration and Acoustics* **114**, 194–208. Investigation on the steady-state responses of asymmetric rotors.
11. V. T. Nagaraj and P. Shanthakumar 1975 *Journal of Sound and Vibration* **43**, 575–577. Rotor blade vibrations by the Galerkin finite element method.
12. S. Putter and H. Manor 1978 *Journal of Sound and Vibration* **56**, 175–185. Natural frequencies of radial rotating beams.
13. S. V. Hoa 1979 *Journal of Sound and Vibration* **67**, 369–381. Vibration of rotating beam with tip mass.
14. Y. A. Khulief and L. Yi 1988 *Computers and Structures* **29**, 1075–1085. Lead–lag vibrational frequencies of a rotating beam with end mass.
15. T. Yokoyama 1988 *International Journal of Mechanical Sciences* **30**, 743–755. Free vibration characteristics of rotating Timoshenko beams.
16. P. J. Magari, L. A. Shultz and V. R. Murthy 1988 *Computers and Structures* **29**, 763–776. Dynamics of helicopter rotor blades.
17. Y. A. Khulief 1989 *Journal of Sound and Vibration* **134**, 87–97. Vibration frequencies of a rotating tapered beam with end mass.
18. A. Bazoune and Y. A. Khulief 1992 *Journal of Sound and Vibration* **156**, 141–164. A finite beam element for vibration analysis of rotating tapered Timoshenko beams.
19. C. Bagci and S. Rajavenkateswaran 1987 *Proceedings of the 5th International Modal Analysis Conference*, 1708. Critical speed and modal analysis of rotating machinery using spatial finite-line element method.
20. A. A. Smaili and M. P. Khetawat 1994 *Mechanism and Machine Theory* **29**, 995–1006. Dynamic modeling of automotive engine crankshafts.
21. M. Geradin and N. Kill 1984 *Engineering Computations* **1**, 52–64. A new approach to finite element modeling of flexible rotors.
22. R. W. Stephenson, K. E. Rouch and R. Arora 1989 *Journal of Sound and Vibration* **131**, 431–443. Modelling of rotors with axisymmetric solid harmonic elements.

23. R. W. Stephenson and K. E. Rouch 1993 *ASME Journal of Vibration and Acoustics* **115**, 484–489. Modeling rotating shafts using axisymmetric solid finite elements with matrix reduction.
24. 1994 *ANSYS User's Manual*, Elements reference.
25. J. S. Rao 1991 *Rotor Dynamics*. New Delhi: Wiley Eastern; second edition.